Indian Journal of Engineering & Materials Sciences
Vol. 32, October 2025, pp. 634-654
DOI: 10.56042/ijems.v32i05.21506

Probabilistic analysis of cracking moment of ferrocement flexural members

K. Balaji Rao[a*] & Prakash Desayi[b]

[a]Centre of Excellence in Climate Sciences, ATRIA University, Bengaluru 560 024, Karnataka, India

[b]Formerly Professor, Department of Civil Engineering, Indian Institute of Science, Bengaluru 560 012, Karnataka, India
(Now 'No More')

Received: 10 July 2025; accepted: 13 September 2025

Characteristic cracking moment equations for the design of ferrocement flexural members are proposed. These are derived based on the results of a detailed Monte Carlo simulation (MCS) studies. In simulation, the strengths of cement mortar and reinforcement and, dimensions of reinforcements and ferrocement members are considered as random variables. The preliminary cross-sections considered for MCS are of realistic dimensions and are those of 37 ferrocement flexural members. The probability density functions of ultimate strengths of weld mesh and steel bars, required in MCS, are determined from the uni-axial tension tests on 187 weld mesh bars, 200 specimens of 4 mm diameter and 80 specimens of 6.8 mm diameter steel bars. Two deterministic equations, proposed earlier by the authors, are used in MCS. It is noted that the statistical variations in compressive strength of cement mortar has significant effect on coefficient of variation of cracking moment, and that the cracking moment follows a normal distribution at 5% significance level. A more rational equation is derived for cumulative distribution function of cracking moment and it satisfies the condition that cracking moment can not be negative. A detailed review of literature on strength and behaviour of ferrocement flexural members is included as supplementary material.

Keywords: Ferrocement, First-crack, Flexure, Monte Carlo simulation, Probabilistic analysis

1 Introduction

Ferrocement is a composite in which brittle cement mortar matrix is reinforced with aligned, ductile fibers[1,2]. Due to extensive research and development carried out, the definition of ferrocement as presented in ACI includes the use of discrete fibres, non-metallic reinforcement such as polymeric reinforcement and textile reinforcement and combinations of these. The code allows flexibility with respect to use of materials by adding "*The fineness of the mortar matrix and its composition should be compatible with the mesh and armature systems it is meant to encapsulate. The matrix may contain discontinuous fibers"*[3] based on the suggestion of Naaman[4].

Being thin elements, they provide flexibility in fabrication and construction. There are number of practical applications of ferrocement for marine and terrestrial structures[viz.5-12]. Ferrocement is also used to develop architecturally and aesthetically appealing structures. Construction of ferrocement water tanks, storage bins, roofing, floor and walling elements are popular[2,13] due to better crack control in ferrocement compared to reinforced concrete.Ferrocement members derive their stiffness and strength owing to their form and, the strengths of mortar and mesh reinforcement used. Also, alignment and the way of distribution mesh wires across the section play important role. One of the important design considerations that governs the serviceability behaviour and the durability of ferrocement flexural elements is the first crack moment. Number of investigations are available in literature dealing with characterisation of strength and behaviour of ferrocement flexural members. While these studies have been reviewed in the supplementary material of this paper, a brief review of literature on ferrocement technology with a focus on recent developments is presented in the following.

Pioneering efforts have been made by Naaman and Shah in understanding the strength and behaviour of Ferrocement over decades[viz. 14-19] and they played a key role in popularising the ferrocement technology by brining out state-of-the-art reports from time to time, and in developing the codes

*Corresponding author (Email: balajiserc@gmail.com, balaji.k@atriauniversityedu.in)

of practice[3,20]. In India also efforts have been made to develop the ferrocement technology[10.11]. Recently, Minde et al.,[21] have shown that ferrocement, as a construction material, is sustainable in the Indian context.

Naaman[18] presented an insightful paper on the development of ferrocement technology involving new methods of analyses and design, use of hybrid composites with ultra high strength mortars and different types of fibres to achieve high strength and ductility. The use of robots in the manufacture of composites was suggested. It was pointed out that the optimization procedure in the design of sustainable and durable ferrocement composites should not only take in to account the mesh-mortar parameters but also other parameters such as those related to production process, the rheology of fresh mix, the properties of hardened composite and final application of material. It is noted that the further developments have followed on similar lines as predicted by Naaman18. These have been made possible due to developments in material science and technology, instrumentation, computational and construction technologies.

Recently, the developments in AI techniques such as ANN, Fuzzy-ANN, GA, ML are being used to develop predictive models for analysis of ferrocement flexural elements and to evolve new composite materials of optimal composition satisfying various constraints. Some of these studies which would be useful in ferrocement research are presented next. The studies presented are only representative and not exhaustive and they point out the future direction of research.

Gandhomi *et al*[22] have proposed a robust variant of genetic expression programming approach to predict the flexural capacity of ferrocement members. This approach falls in the realm of artificial intelligence techniques and will be useful for modelling phenomena exhibiting large variations. Using an intelligent variant of polynomial fitting of test results of ferrocement flexural members, Naderpour *et al*[23] proposed a group method of handling data. The expression for ultimate moment carrying capacity obtained using the proposed method predicted the experimental results in literature better than the once proposed by Gandhomi *et al*[22].Behnia *et al*[24] integrated machine learning techniques with the AE signal analysis to predict the progressive damage and to carry out reliability analysis using hazard rate function for multi-layer ferrocement slabs tested under monotonically increasing loads.

Pyzer-Knapp *et al*[25] bring out the importance of AI, high performance computing and robotics in accelerating the materials discovery. Li et al[26] presented an informative general work flow of ML in concrete science (Fig. 4 of Ref.26) in which the importance of relevant data from literature, experiments and simulations has been brought out. A comprehensive survey of application of AI techniques in concrete technology for the period 2013 – 2023 was presented by Kazemi[27]. This paper clearly brings out the importance of test data for use in application of AI techniques. It is possible to apply similar techniques in ferrocement technology.

However, to apply these advanced techniques for evolving predictive models, creation of a valid database of experimental results coupled with calibrated simulation results are required.

Based on the review presented above and that presented in the supplementary material it has been noted that there is a need to carry out probabilistic analysis of ferrocement flexural elements and also there is an urgent need to create a very detailed database of test results on ferrocement flexural members. Keeping these in view the studies reported in this paper are carried out.

As has been pointed out by Naaman[4]the main reason for the lack of progress in practice of ferrocement technology is due to the absence of a widely accepted and updated building code for the design and construction of ferrocement structures. Development of such a code will help the public, armature and self-help builders. Also, development of probability-based design clauses would help in the development of LRFD code.

Recently Desayi and Balaji Rao[35] and Balaji Rao and Desayi[36,37] reported the results of probabilistic analyses of frist-crack and ultimate strengths of normal and light weight ferrocement elements under axial tension. This paper focuses on determination of characteristic first crack strength of ferrocement flexural elements within the probabilistic framework, which is a step towards development of LRFD code. Also, the details of experimental work carried out in the Structural Engineering laboratory of IISc on ferrocement flexural elements are presented in detail so that these test results can be included in a suitable database for futuristic studies on application of ML techniques for prediction of cracking moment.

2 Materials and Methods

2.1 Flexural tests on ferrocement roofing and floor elements and, built-up and monolithic I-joists

Number of studies dealing with experimental tests on ferrocement flexural members have been reported in the literature (a review of relevant literature is presented in the supplementary material associated with this paper). However, tests on specimens of size generally used in practice are scanty. The test data of 37 ferrocement flexural elements comprising 6 roofing elements of trapezoidal cross-section, 9 floor elements of channel cross-section, and ferrocement joists consisting of 16 built-up I-sections and 6 monolithic I-sections are considered in this investigation. The tests were carried out in the Structural Engineering Laboratory of Indian Institute of Science. Bengaluru[28-33]. The cross-sectional details, loading details, strengths of mortar, mesh wires, weld mesh/steel bars, reinforcement details are presented in Tables 1 -4. Some of the notation used in these tables are explained in Figs. 1- 3. Table 4 also presents the experimentally observed cracking

Table 1 — Cross-sectional dimensions of roofing and floor elements, and built-up I-sections (also see Figs 1 – 3)

Type of cross-section	Specimen designation	Effective span (L) (mm)	L/D ratio	b_1 (mm)	t_1 (mm)	b_2 (mm)	t_2 (mm)	d_w (mm)	t_w (mm)
Trapezoidal roofing elements[29]	K20-422	3400	20	210	20	235	20	130	56.6
	K20-622	3400	20	210	20	235	20	130	56.6
	K15-422	3600	15	210	20	235	20	200	56.6
	K15-622	3600	15	210	20	235	20	200	56.6
	K10-422	3200	10	210	20	235	20	280	56.6
	K10-622	3200	10	210	20	235	20	280	56.6
Channel type floor elements[28.31]	F1	2500	10	500	20	-	-	230	50
	F2	2500	10	500	20	-	-	230	50
	F3	2500	10	500	20	-	-	230	50
	F4	3000	12	500	20	-	-	230	50
	F5	3000	12	500	20	-	-	230	50
	F6	3000	12	500	20	-	-	230	50
	F7	3500	14	500	20	-	-	230	50
	F8	3500	14	500	20	-	-	230	50
	F9	3500	14	500	20	-	-	230	50
Built-up I-sections of Group I[30,32]	S1	1200	11.32	106	19.0	106	19.0	68	36
	S2	1200	11.32	106	19.0	106	19.0	68	36
	S3	1200	11.32	106	19.0	106	19.0	68	36
	S4	1200	8.0	150	20.0	150	20.0	110	40
	S5	1200	8.0	150	25.0	150	25.0	100	50
	S6	1200	6.0	200	20.5	200	20.5	159	50
	S7	1200	6.0	200	30.0	200	30.0	140	60
Built-up I-sections of Group II[30.32]	A1	2000	10	120	30	120	30	140	40
	A2	2400	12	120	30	120	30	140	40
	A3	2800	14	120	30	120	30	140	40
	B1	2500	10	150	30	150	30	190	40
	B2	3000	12	150	30	150	30	190	40
	B3	3500	14	150	30	150	30	190	40
	C1	3000	10	180	30	180	30	240	40
	C2	3600	12	180	30	180	30	240	40
	C3	4200	14	180	30	180	30	240	40

(*Contd.*)

Table 1 — Cross-sectional dimensions of roofing and floor elements, and built-up I-sections (also see Figs 1 – 3) (*Contd.*)

Type of cross-section	Specimen designation	Effective span (L) (mm)	L/D ratio	b_1 (mm)	t_1 (mm)	b_2 (mm)	t_2 (mm)	d_w (mm)	t_w (mm)
Monolithic I-Sections[33,34]	MI1	2300	2000	200	10	120	30	140	30
	MI2	3100	2800	200	14	120	30	140	30
	MI3	2800	2500	250	10	150	30	190	30
	MI4	3800	3500	250	14	150	30	190	30
	MI5	3300	3000	300	10	180	30	240	30
	MI6	4500	4200	300	14	180	30	240	30

Table 2 — Reinforcement used in ferrocement elements and their strength details

Type of cross-section	Type of reinforcement	Gauge/spacing	Diameter (mm)	Modulus of elasticity (N/mm^2)	Proof stress (N/mm^2)	Ultimate stress (N/mm^2)
Trapezoidal roofing elements[29]	Steel bars	-	6.80	228573	398.29	521.40
	Woven mesh	4 x 22	0.71	16088.4	325.30	393.38
	Woven mesh	6 x 22	0.71	16088.421	325.30	393.38
Channel type floor elements[28,31]	High strength plain bars	-	4.0	215035.2	681.80	703.87
	High strength plain bars	-	6.8	244955.7	529.74	581.24
	Woven mesh wire	4 x 22	0.70	NA	325.30	393.23
Built-up I-sections of Group I[30,32]	Weld mesh	25.4 mm x 50.8 mm	-	191981.7	828.95	871.13
	Weld mesh*	25.4 mm X 25.4 mm	-	211896	470.88	490.50
	Weld mesh**	25.4 mm X 25.4 mm	-	130080.6	600.86	610.18
	Chicken wire mesh	24 (gauge)	0.50	246623.4	484.61	496.39
Built-up I-sections of Group II[30,32]	Weld mesh	25.4 mm X 25.4 mm	2.54	130080.6	600.86	610.18
	Wire mesh	4 x 22	0.57	259376.4	325.30	393.38
	Wire mesh	4 x 20	0.76 mm	8240.4	498.35	575.46
Monolithic I-Sections[33,34]	Wire mesh	4 x 22	0.61 mm	12949.2	392.40	465.98
	Weld mesh	25.4 mm X 25.4 mm	2.54 mm	130080.6	600.86	610.18

Note: * Weld mesh cut out of first roll, ** Weld mesh cut out of second roll;

Table 3 — Reinforcement details of roofing and floor elements, and built-up and monolithic I - joists

Type of cross-section	Specimen designation	Wire mesh type	Weld mesh/Steel bar type	Number of mesh wires running in longitudinal direction		Number of weld mesh bars/steel bars running in longitudinal direction	
				Each flange	web	Each flange	Web
Trapezoidal roofing elements[29]	K20-422	4/22	6.8 mm dia. bars	134	136	8	2
	K20-622	6/22	6.8 mm dia. bars	200	204	8	2
	K15-422	4/22	6.8 mm dia. bars	134	198	9	4
	K15-622	6/22	6.8 mm dia. bars	200	298	9	4
	K10-422	4/22	6.8 mm dia. bars	134	270	10	6
	K10-622	6/22	6.8 mm dia. bars	200	404	10	6
Channel type floor elements[28,31]	F1	4/22	4 mm dia. bars and 6.8 mm dia. bars	156	138	5 (4 mm dia) - (6.8 mm dia)	2 (4 mm dia) 2 (6.8 mm dia)
	F2	4/22	4 mm dia. bars and 6.8 mm dia. bars	156	138	3 (4 mm dia) 2 (6.8 mm dia)	2 (4 mm dia) 4 (6.8 mm dia)
	F3	4/22	4 mm dia. bars and 6.8 mm dia. bars	156	138	- (4 mm dia) 5 (6.8 mm dia)	2 (4 mm dia) 6 (6.8 mm dia)
	F4	4/22	4 mm dia. bars and 6.8 mm dia. bars	156	138	5 (4 mm dia) - (6.8 mm dia)	2 (4 mm dia) 2 (6.8 mm dia)
	F5	4/22	4 mm dia. bars and 6.8 mm dia. bars	156	138	3 (4 mm dia) 2 (6.8 mm dia)	2 (4 mm dia) 4 (6.8 mm dia)

(*Contd.*)

Table 3 — Reinforcement details of roofing and floor elements, and built-up and monolithic I – joists (*Contd.*)

Type of cross-section	Specimen designation	Wire mesh type	Weld mesh/Steel bar type	Number of mesh wires running in longitudinal direction		Number of weld mesh bars/steel bars running in longitudinal direction	
				Each flange	web	Each flange	Web
	F6	4/22	4 mm dia. bars and 6.8 mm dia. bars	156	138	- (4 mm dia) 5 (6.8 mm dia)	2 (4 mm dia) 6 (6.8 mm dia)
	F7	4/22	4 mm dia. bars and 6.8 mm dia. bars	156	138	5 (4 mm dia) - (6.8 mm dia)	2 (4 mm dia) 2 (6.8 mm dia)
	F8	4/22	4 mm dia. bars and 6.8 mm dia. bars	156	138	3 (4 mm dia) 2 (6.8 mm dia)	2 (4 mm dia) 4 (6.8 mm dia)
	F9	4/22	4 mm dia. bars and 6.8 mm dia. bars	156	138	- (4 mm dia) 5 (6.8 mm dia)	2 (4 mm dia) 6 (6.8 mm dia)
Built-up I-sections of Group I[30,32]	S1	Chicken mesh (24 gauge)	25.4 x 50.8 mm	12	12	3	2
	S2	Chicken mesh (24 gauge)	25.4 x 25.4 mm*	12	12	4	4
	S3	Chicken mesh (24 gauge)	25.4 x 50.8 mm	12	12	3	2
	S4	Chicken mesh (24 gauge)	25.4 x 25.4 mm**	14	20	6	8
	S5	Chicken mesh (24 gauge)	25.4 x 25.4 mm**	18	16	7	6
	S6	Chicken mesh (24 gauge)	25.4 x 25.4 mm**	20	32	8	12
	S7	Chicken mesh (24 gauge)	25.4 x 25.4 mm*	20	28	8	12
Built-up I-sections of Group II[30,32]	A1	4/22	25.4 x 25.4 mm	40	88	6	10
	A2	4/22	25.4 x 25.4 mm	40	88	6	10
	A3	4/22	25.4 x 25.4 mm	40	88	6	10
	B1	4/22	25.4 x 25.4 mm	48	120	6	14
	B2	4/22	25.4 x 25.4 mm	48	120	6	14
	B3	4/22	25.4 x 25.4 mm	48	120	6	14
	C1	4/22	25.4 x 25.4 mm	56	48	8	18
	C2	4/22	25.4 x 25.4 mm	56	48	8	18
	C3	4/22	25.4 x 25.4 mm	56	48	8	18
Monolithic I-Sections[33,34]	MI1	4/20	25.4 mm x 25.4 mm	30	46	6	6
	MI2	4/20	25.4 mm x 25.4 mm	30	46	6	6
	MI3	4/22	25.4 mm x 25.4 mm	38	56	7	7
	MI4	4/22	25.4 mm x 25.4 mm	38	56	7	7
	MI5	4/20	25.4 mm x 25.4 mm	54	76	8	9
	MI6	4/22	25.4 mm x 25.4 mm	54	76	8	9

Note: * Weld mesh cut out of first roll, ** Weld mesh cut out of second roll;

Table 4 — Strength details of mortar and ferrocement roofing and floor elements, and, built-up and monolithic I-joists.

Type of cross-section	Specimen designation	Compression strength of mortar cube (N/mm^2)	Modulus of rupture of mortar (N/mm^2)	Distance of load point from the support (mm)	Cracking moment of the specimen (kN-mm)
Trapezoidal section roofing elements[29]	K20-422	36.00	3.53	1133.30	3192.133
	K20-622	35.41	3.14	1133.30	3353.911
	K15-422	31.98	3.14	1200.00	4374.781
	K15-622	38.06	3.34	1200.00	5368.385

(*Contd.*)

Table 4 — Strength details of mortar and ferrocement roofing and floor elements, and, built-up and monolithic I-joists. (*Contd.*)

Type of cross-section	Specimen designation	Compression strength of mortar cube (N/mm^2)	Modulus of rupture of mortar (N/mm^2)	Distance of load point from the support (mm)	Cracking moment of the specimen (kN-mm)
	K10-422	31.59	4.22	1066.70	7325.271
	K10-622	39.73	3.92	1066.70	12180.986
Channel type floor elements[28,31]	F1	52.38	3.83	833.30	5084.482
	F2	52.48	2.94	833.30	7160.937
	F3	34.34	3.24	833.30	6686.781
	F4	44.73	3.53	1000.00	6240.632
	F5	48.46	4.71	1000.00	3748.892
	F6	38.16	5.49	1000.00	6240.632
	F7	36.40	4.51	1166.70	4485.328
	F8	44.05	3.63	1166.70	4485.289
	F9	46.01	4.61	1166.70	4485.328
Built-up I-sections of Group I[30,32]	S1	22.56	2.82	400.00	638.827
	S2	24,53	2.35	400.00	585.049
	S3	21.19	2.65	400.00	422.987
	S4	24.53	2.16	400.00	1180.624
	S5	25.02	2.35	400.00	1180.221
	S6	25.02	2.35	400.00	2520.679
	S7	24.53	2.35	400.00	2550.541
Built-up I-sections of Group II[30,32]	A1	19.17	3.14	750.00	1476.908
	A2	18.58	3.05	800.00	1626.498
	A3	22.32	3.42	933.00	2071.469
	B1	17.75	2.12	833.00	2662.905
	B2	30.30	3.94	1000.00	3381.997
	B3	27.66	2.70	1166.00	3267.642
	C1	14.10	2.22	1100.00	4753.043
	C2	14.40	2.50	1300.00	4549.633
	C3	14.58	2.72	1400.00	4010.328
Monolithic I-Sections[33,34]	MI1	31.43	2.80	670	2392.552
	MI2	23.17	3.39	920	1550.598
	MI3	27.72	2.29	870	4071.415
	MI4	21.64	2.01	1170	2184.589
	MI5	29.78	2.29	1000	4350.343
	MI6	32.25	2.51	1400	5514.691

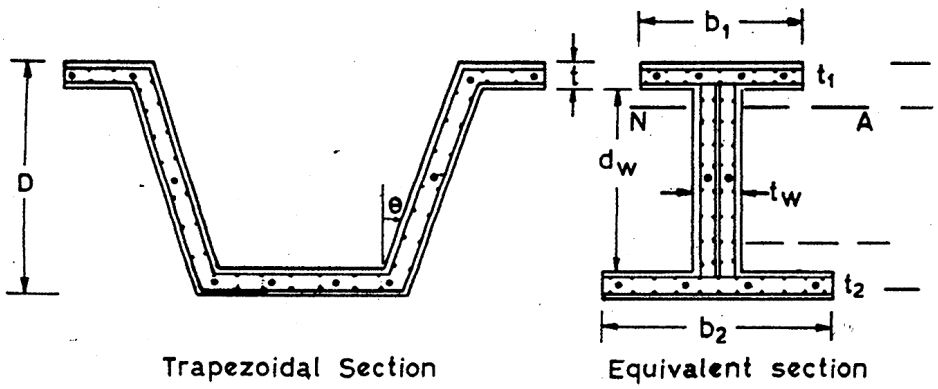

Fig. 1 — Trapezoidal roofing elements – Actual cross-section and its equivalent section.

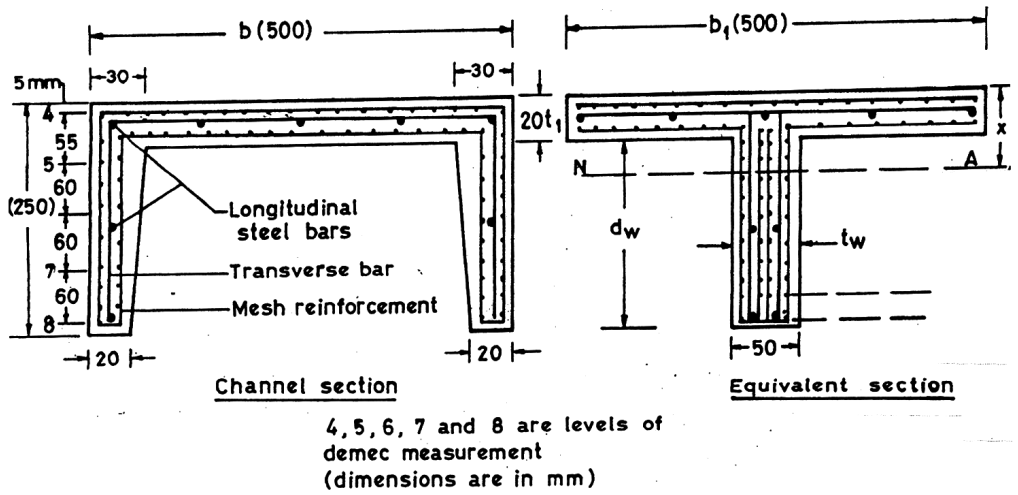

Fig. 2 — Channel type floor elements – Actual cross-section and its equivalent section.

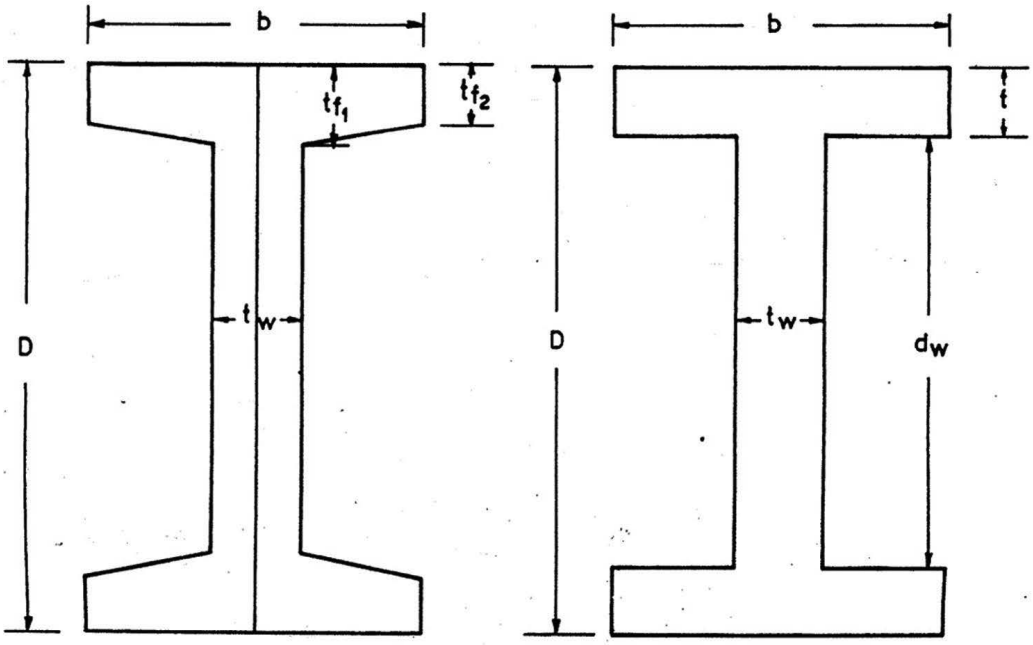

Fig. 3 — I Section – Actual cross-section and its equivalent section $t = \frac{t_{f1}+t_{f2}}{2}$.

moments of 37 elements. Using the details presented in Tables 1 - 4, two methods proposed earlier by the authors[34], are presented briefly in the next section for the sake of completeness of this paper. These deterministic models are further used to carry out probabilistic analysis of cracking moment using Monte Carlo simulation (MCS).

2.2 Deterministic models to predict the cracking moment (M_{cr}) of ferrocement elements

The authors have proposed two methods[34], for the prediction of M_{cr}. While the first method is based on reinforced concrete theory, the second method takes into account mesh-mortar contribution through mesh-mortar parameter.

2.2.1 Method – I

According to this method, the first crack strength of ferrocement element is given by

$$M_{cr} = \frac{f_r I_g}{y_b} \quad \ldots (1)$$

Where f_r is the modulus of rupture of cement mortar, I_g is the moment of inertia of gross-transformed

equivalent sections for roofing and floor elements (Figs. 1 and 2), and, moment of inertia of gross section in case of built-up and monolithic I-sections (Fig. 3), and $y_b$is the distance of extreme tension fibre from centroidal axis of the section. The modulus of rupture of the cement mortar is obtained from the Eq. (2). This relationship is obtained from the linear regression analysis of $\sqrt{f_{cu}}$ vs f_r of the test data of 37 specimens considered in this study. The plot is shown in Fig. 4. In this plot each point corresponds to the average of three cubes and three prisms of the corresponding flexural member. From the regression analysis the following relation is obtained.

$$f_r = 0.57\sqrt{f_{cu}} \text{ MPa} \quad \ldots (2)$$

2.2.2 Method – II

This method is similar to Method I, except that the presence of wire meshe in the cross-section is also considered. Accordingly,

$$M_{cr} = \frac{f_{rm}\, I_g}{y_b} \quad \ldots (3)$$

Where f_{rm} is the modulus of rupture of mesh-mortar combination and is obtained from Eq. (2) in which f_{cu} is replaced with f_{cm} (mesh-mortar cube strength). The value of f_{cm} is obtained from

$$\frac{f_{cm}}{f_{cu}} = \left[1 + 1.095\,\frac{p_m f_{su}}{f_{cu}}\right] \quad \ldots (4)$$

Where p_m is the ratio of the area of wires in the longitudinal direction to the area of cross-section and f_{su} is the ultimate strength of mesh wires. I_g and y_b are as defined in Method – I.

By comparing the values of cracking moment obtained from Methods I and II with the respective experimental results of 37 specimens the ratio of estimated to experimental cracking moments was found to be 0.866 and 0.892, respectively. The coefficient of variation of the ratios are approximately the same and are around 22%.The details of comparison are not presented here since the focus is on probabilistic analysis. It is noted that the Method – II gives slightly better agreement with the experimental values (COV of both the methods being almost the same) and it takes in to account the mesh-mortar contribution towards cracking moment.

In order to carry out the probabilistic analysis, the probability density functions of basic variables are required. Keeping this in view, tests have been carried

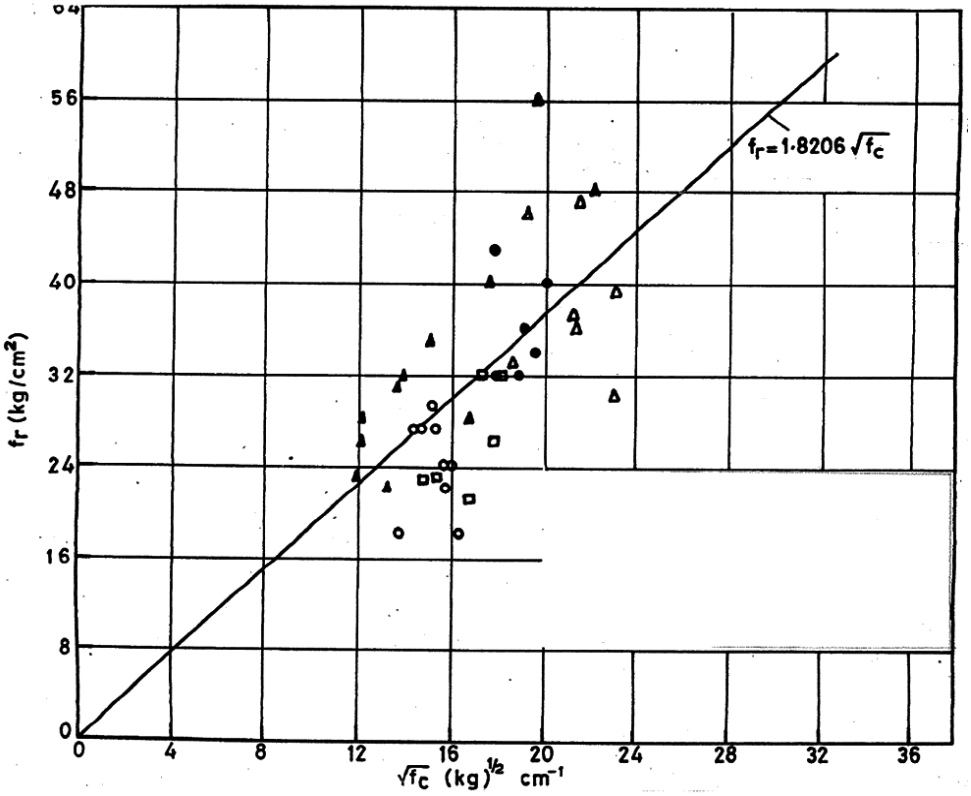

Fig. 4 — Relationship between modulus of rupture and compressive strength of cement mortar.

on wire mesh and weld mesh wires and steel bars used in the 37 flexural members. Desayi and Balaji Rao38 have reported the statistical properties of wire mesh wires of 4/20 and 6/22 meshes based on the tests conducted by them. Also, in literature on reinforced concrete while the information about the distributions followed by diameter and ultimate strength of steel bars are available, the same are not available for weld mesh bars and steel bars used in this investigation. Hence, tension tests were conducted in the laboratory of Indian Institute of Science, on weld mesh bars and steel bars of 4 mm and 6.8 mm (nominal) diameter. The details of this study are presented next.

2.3 Tension tests on Weld Mesh and Steel Bars

The test programme consisted of testing a total of 467 specimens in uni-axial tension. Out of these, 187 specimens were of weld mesh bars, 200 specimens of 4 mm diameter and 80 specimens of 6.8 mm diameter steel bars. The bars of each type were divided into two groups, namely, Group 1 and Group 2, since they were cut from two different rolls (received from different sources). The number of bars of each type in a given group is presented in Table 5. Each bar was of 1000 mm length and was tested in an universal testing machine of 996.7 kN capacity. Before testing, the diameter of each bar was measured at three different locations and the average diameter was taken as the representative value for that bar. The ultimate strength of the bar was calculated based on the average diameter. Almost all the bars failed nearer to the central section, and, a cup and cone fracture was observed at failure. This suggests that the failure of weld mesh and steel bars are ductile in nature.

2.3.1 Distribution of diameter of bars

From the experimental data, the statistical properties, namely, mean, standard deviation, coefficient of variation, and coefficients of skewness and kurtosis of the distribution of diameter of weld mesh and steel bars belonging to Groups 1 and 2 were computed and their values are presented in Table 5. It can be noted from this table that for a given type of reinforcement, there is a small difference in the mean values of diameter of bars belonging to Group 1 and Group 2 and the difference in the coefficient of variation of diameters is insignificant. By comparing the coefficients of variation of diameter of weld mesh bars with that of mesh wires, presented in Desayi and Balaji Rao[38], it is found that the coefficient of variation of the former is less than that of the latter (which is in the range of 0.037 to 0.080). From Chi-square goodness-of-fit tests[39] it was found that both normal and lognormal distribution failed to satisfy the test criteria at 5% significance level[33]. However, in the present investigation diameters of mesh wires, weld mesh and steel bars are assumed to follow normal distribution since this distribution is commonly used to describe the variations in dimensions[40-44].

2.3.2 Distribution of ultimate strength of bars

From the test data of ultimate strengths of weld mesh bars and steel bars, statistical properties namely, mean, coefficient of variation, and, coefficients of skewness and kurtosis are computed for different groups and are presented in Table 5. Histograms are plotted to determine the nature of variability of ultimate strength. Using this information cumulative frequency distributions have been obtained. These are

Table 5 — Statistical properties of diameter and ultimate tensile strength of weld mesh bars and steel bars (tests conducted in this study)

Material	Variable under study	Group	Number of specimens	Mean	SD	COV	SK	CU
Weld mesh bars	Diameter	Group 1	100	2.334 mm	0.016 mm	0.007	0.000	1.710
		Group 2	87	2.388 mm	0.011 mm	0.005	1.507	6.301
	Ultimate strength	Group 1	100	622.050 MPa	86.760 MPa	0.139	-1.020	4.760
		Group 2	87	938.920 MPa	169.030 MPa	0.180	-0.008	2.380
4 mm diameter steel bars	Diameter	Group 1	100	4.127 mm	0.005 mm	0.001	0.213	3.868
		Group 2	100	4.039 mm	0.004 mm	0.001	0.630	3.680
	Ultimate strength	Group 1	100	824.350 MPa	17.91 MPa	0.022	0.340	4.330
		Group 2	100	729.970 MPa	19.93 MPa	0.027	-0.230	2.930
6.8 mm diameter steel bars	Diameter	Group 1	47	7.236 mm	0.078 mm	0.011	-0.475	3.065
		Group 2	33	7.119 mm	0.075 mm	0.011	1.125	10.697
	Ultimate strength	Group 1	47	550.690 MPa	15.67 MPa	0.029	0.640	5.100
		Group 2	33	448.920 MPa	10.96 MPa	0.024	1.290	8.700

shown in Figs. 5-7. In order to determine the actual distribution followed by ultimate strength, Chi-square goodness-of-fit tests are performed. Three distributions considered for the goodness-of-fit tests are normal, lognormal and beta (of the first kind). The final Chi-square test results of weld mesh bars and steel bars (of Groups 1 and 2) are presented in Table 6. In Table 6, the degrees of freedom related to Chi-square test are also provided. By comparing the computed Chi-square values with the allowable values for given degrees of freedom and significance level the following points are noted:

(i) At 97.5% confidence level normal and beta distributions pass the Chi-square test for weld mesh bars of Group 1 while lognormal and beta distributions pass the test for weld mesh bars of Group 2.

(ii) In case of 4 mm diameter steel bars belonging to Group 1 all the three assumed distributions pass the Chi-square test at 95% confidence level while in case of those belonging to Group 2 none of the distributions pass the Chi-square test at 95% confidence level.

(iii) Normal, lognormal and beta distributions pass the Chi-square test criterion at 95% confidence level

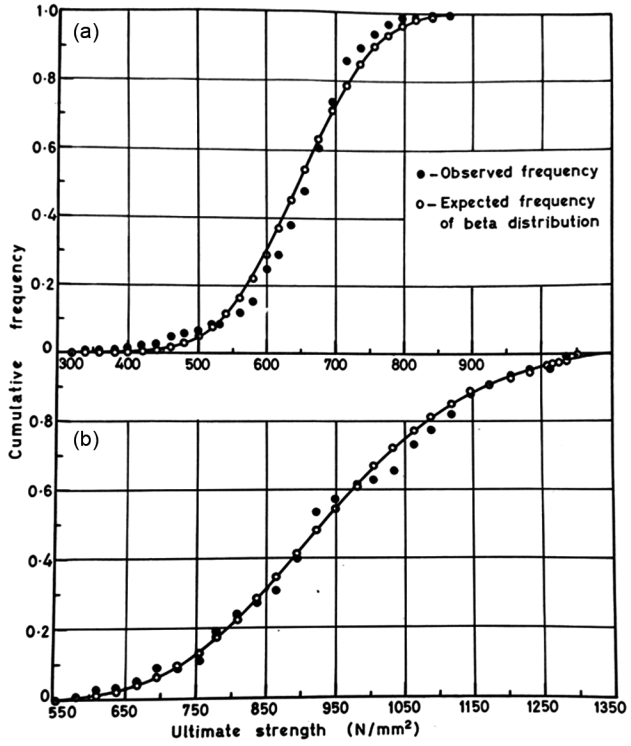

Fig. 5 — Cumulative distribution functions of ultimate strengths of weld mesh bars of (a) Group 1, and (b) Group 2.

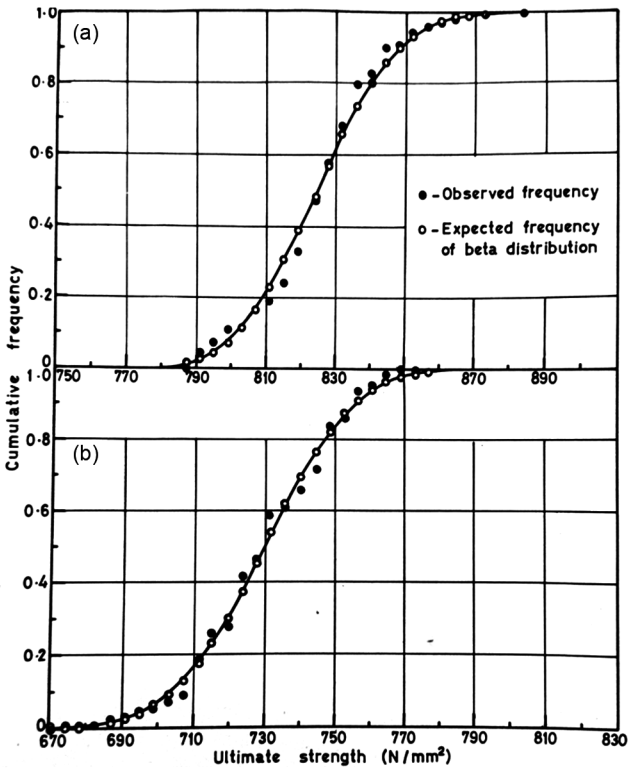

Fig. 6 — Cumulative distribution functions of ultimate strengths of 4 mm diameter steel bars of (a) Group 1, and (b) Group 2.

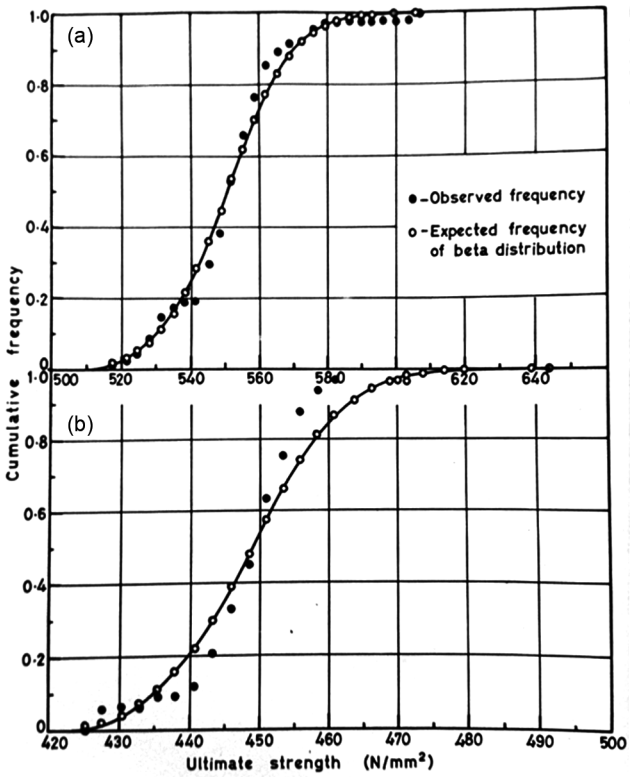

Fig. 7 — Cumulative distribution functions of ultimate strengths of 6.8 mm diameter steel bars of (a) Group 1, and (b) Group 2.

Table 6 — Chi-square test result* for ultimate strength of weld mesh bars and steel bars (tests conducted in this study)

Material	Group	Chi-square values for different hypothetical distributions		
		Normal	Lognormal	Beta
Weld mesh bars	Group 1	19.924 (10)	26.184 (10)	19.316 (10)
	Group 2	22.458 (10)	20.170 (11)	20.541 (11)
4 mm diameter steel bars	Group 1	13.357 (12)	13.030 (11)	15.710 (11)
	Group 2	31.337 (11)	31.805 (11)	29.893 (10)
6.8 mm diameter steel bars	Group 1	6.369 (4)	6.665 (4)	6.337 (4)
	Group 2	6.885 (3)	6.892 (3)	6.894 (3)

* - The values in the brackets indicate the degrees of freedom used in the test

in case of 6.8 mm diameter steel bars belonging to both Groups 1 and 2.

In literature, to describe the statistical variation in ultimate strength of steel bars, some investigators[42] report that normal distribution can be used while the others[45] use beta distribution. In the present investigation beta distribution of the first kind is finally chosen for ultimate strength of weld mesh bars and steel bars, since this is one of the basic distributions that can be used when random variable is bounded on both the sides (which renders it more suitable than normal or lognormal distributions). In Figs. 5-7, the expected cumulative frequencies of beta distribution are superimposed over the observed cumulative frequencies for the purpose of comparison. From these figures it can be seen that the expected and observed cumulative frequencies agree satisfactorily for different values of ultimate strength (a random variable). The agreement is better for smaller values of ultimate strength. This shows that the beta distribution can be used to fit the lower tails of ultimate strength distribution; which is of importance in the estimation of reliability of ferrocement flexural elements. The parameters of the beta distribution can be estimated using the values of mean and variance of ultimate strength[39]. Having known the distributions of the basic random variables, probabilistic analysis of the cracking moment can now be carried out. This is presented in the next section.

2.4 Probabilistic analysis of cracking moment

Due to variations in cross-sectional dimensions and strengths of materials used, the cracking moment (M_{cr}) of a ferrocement element is a random variable. This section aims at the determination of statistical properties of M_{cr} using Monte Carlo simulation technique. The deterministic models used to predict the M_{cr} are the Methods I and II presented in Section 4. In the analysis all the basic quantities appearing in Eqs. (1) and (3) are treated as random variables. The basic variables considered together with their distributions are presented in Table 7. The preliminary sections considered for the probabilistic analysis are 37 specimens tested in the Structural Engineering laboratory if IISc; whose details are presented in Tables 1 – 4 and Figs. 1 – 3. One thousand values are generated for each of the random variables presented in Table 7. Using these values random cracking moments are generated for each of the 37 specimens. This exercise is repeated for both Methods I and II for a given specimen. Thus, for a given flexural specimen there are one thousand random cracking moment values for each of the Methods used. The statistical properties of cracking moment are determined from the following equations:

$$\bar{X} = \frac{1}{N}\sum_{i=1}^{N} m_i \quad \ldots (5)$$

$$S^2 = \frac{1}{(N-1)}\sum_{i=1}^{N}(m_i - \bar{X})^2 \quad \ldots (6)$$

$$COV = \frac{S}{\bar{X}} \quad \ldots (7)$$

$$SK = \frac{1}{NS^3}\sum_{i=1}^{N}(m_i - \bar{X})^3 \quad \ldots (8)$$

$$CU = \frac{1}{NS^4}\sum_{i=1}^{N}(m_i - \bar{X})^4 \quad \ldots (9)$$

where m_i, is the i^{th} cracking moment value, $\bar{X}$is the mean cracking moment, $S^2$is the variance, COV is the coefficient of variation, *SK* is the skewness coefficient, and *CU* is the kurtosis of cracking moment. In the present investigation N = 1000. It is noted that using 1000 simulation cycles, the lengths of two-sided 95% confidence intervals for population mean and variance are 0.1240S and 0.1762S^2, respectively.

Table 7 — Variables considered in the study and their distribution

Variable	Mean	Coefficient of variation	Distribution	Reference
Dimensions (width, depth, thickness)	Actual dimension	0.03	Normal	40-44
Diameter of mesh wires				
4/22	Experimental value	0.04	Normal	
6/22	Experimental value	0.04	Normal	35,36
4/20	Experimental value	0.07	Normal	
Diameter of weld mesh bars	Experimental value	0.007	Normal	Section 5.1
Diameter of steel bars				
6.8 mm (nominal)	Experimental value	0.011	Normal	Section 5.1
4.0 mm (nominal)	Experimental value	0.001	Normal	
Strengths of mesh wires 6/22 and 4/22	Experimental ultimate strength	Shape parameter (γ) = 15.1343 Scale parameter = $\frac{Mean}{\left(\frac{1}{\gamma}+1\right)}$	Weibull	38
Strength of mesh wire 4/20	Experimental ultimate strength	Shape parameter (γ) = 11.8645 Scale parameter = $\frac{Mean}{\left(\frac{1}{\gamma}+1\right)}$	Weibull	38
Strength of weld mesh bars	Experimental ultimate strength			
	For 450 MPa – 600 MPa	0.1395	Beta	Section 5.2
	For 800 MPa – 900 MPa	0.1800	Beta	(this study)
Strength of steel bars				
6.8 mm (nominal)	Experimental value	0.029	Beta	Section 5.2
4.0 mm (nominal)	Experimental value	0.027	Beta	(this study)
Modulus of elasticity of weld mesh bars	Experimental value	0.024	Normal	40-44
Modulus of elasticity of steel bars	Experimental value	0.024	Normal	40-44
Cube compressive strength:				
Trapezoidal roofing elements	Experimental value	0.1404[(a)]	Normal	43,44
Channel cross-section floor elements	Experimental value	0.1504[(a)]	Normal	43,44
Built-up I-sections of Group I	Experimental value	0.0976[(a)]	Normal	43,44
Built-up I-sections of Group II*	Experimental value	0.1020 (for series A) 0.2620 (for series B) 0.0170 (for series C)	Normal	43,44
Monolithic I-sections	Experimental value	0.1943[(a)]	Normal	43,44

* - since the coefficient of variation of compressive strength of mortar varied from one series to another, its actual value is used.
(a) –based on experimental test data

2.4.1 Results of probabilistic analysis and discussion

The statistical properties of cracking moment, namely, mean ($\bar{X}$), standard deviation (S), coefficient of variation (COV), coefficients of skewness (SK) and kurtosis (CU) are determined, using Eqs. (5) – (9), for *Methods* I and II and are presented in Tables 8 –12 (in these tables the values presented within brackets represent those obtained using Method II). The results obtained are discussed next.

Table 8 — Comparison of the results of probabilistic analysis of cracking moment* with the experimental values for trapezoidal cross-section roofing elements[29]

Specimen designation	Experimental cracking moment $(M_{cr})_{exp}$ (kN-mm)	Mean cracking moment $(\bar{X})$ (kN-mm)	Coefficient of variation	SK	CU	$\left(\frac{\bar{X}-1.64S}{(M_{cr})_{exp}}\right)$	$\left(\frac{\bar{X}}{(M_{cr})_{exp}}\right)$	$\left(\frac{\bar{X}+1.64S}{(M_{cr})_{exp}}\right)$
K20-422	3192.133	2556.709 (2912.533)	0.160 (0.153)	0.237 (0.235)	3.089 (3.081)	0.591 (0.682)	0.801 (0.912)	1.011 (1.141)
K20-622	3353.911	2535.696 (2897.397)	0.160 (0.152)	0.237 (0.235)	3.089 (3.081)	0.558 (0.648)	0.756 (0.864)	0.954 (1.080)
K15-422	4374.781	4144.682 (4772.327)	0.159 (0.151)	0.237 (0.235)	3.089 (3.081)	0.700 (0.821)	0.947 (1.091)	1.195 (1.361)
K15-622	5368.385	4517.749 (5128.578)	0.159 (0.152)	0.237 (0.235)	3.089 (3.081)	0.622 (0.718)	0.842 (0.955)	1.061 (1.193)
K10-422	7325.271	6492.080 (7487.782)	0.159 (0.151)	0.237 (0.235)	3.089 (3.081)	0.656 (0.770)	0.886 (1.022)	1.117 (1.274)
K10-622	12180.986	7266.280 (8229.659)	0.159 (0.151)	0.237 (0.235)	3.089 (3.081)	0.441 (0.508)	0.597 (0.676)	0.752 (0.843)
Mean (of 6 specimens)						0.595 (0.691)	0.805 (0.920)	1.015 (1.149)
Average COV (of 6 specimens)						0.151 (0.157)	0.151 (0.157)	0.151 (0.156)

* - Values presented in brackets correspond to those obtained using Method II (Eq. 3)

Table 9 — Comparison of the results of probabilistic analysis of cracking moment* with the experimental values for channel cross-section floor elements[28,31]

Specimen designation	Experimental cracking moment $(M_{cr})_{exp}$ (kN-mm)	Mean cracking moment $(\bar{X})$ (kN-mm)	Coefficient of variation	SK	CU	$\left(\frac{\bar{X}-1.64S}{(M_{cr})_{exp}}\right)$	$\left(\frac{\bar{X}}{(M_{cr})_{exp}}\right)$	$\left(\frac{\bar{X}+1.64S}{(M_{cr})_{exp}}\right)$
F1	5084.482	3528.045 (3525.477)	0.158 (0.160)	0.235 (0.235)	3.090 (3.089)	0.520 (0.511)	0.701 (0.693)	0.882 (0.876)
F2	7160.937	3774.786 (3834.307)	0.152 (0.153)	0.233 (0.237)	3.088 (3.085)	0.396 (0.402)	0.527 (0.535)	0.658 (0.669)
F3	6686.781	3410.465 (3499.443)	0.143 (0.145)	0.230 (0.235)	3.085 (3.081)	0.390 (0.399)	0.510 (0.523)	0.630 (0.648)
F4	6240.632	3286.751 (3357.848)	0.157 (0.155)	0.234 (0.238)	3.090 (3.086)	0.394 (0.401)	0.530 (0.538)	0.667 (0.675)
F5	3748.892	3655.469 (3432.924)	0.151 (0.156)	0.233 (0.239)	3.088 (3.087)	0.733 (0.682)	0.975 (0.916)	1.217 (1.150)
F6	6240.632	3549.039 (3630.709)	0.144 (0.146)	0.231 (0.235)	3.085 (3.081)	0.434 (0.442)	0.569 (0.582)	0.703 (0.721)
F7	4485.328	2998.896 (3077.722)	0.156 (0.154)	0.234 (0.239)	3.089 (3.085)	0.498 (0.513)	0.669 (0.686)	0.840 (0.859)
F8	4485.289	3515.142 (3295.836)	0.151 (0.155)	0.233 (0.239)	3.087 (3.086)	0.590 (0.548)	0.784 (0.735)	0.977 (0.922)
F9	4485.328	3806.941 (3881.805)	0.146 (0.148)	0.232 (0.235)	3.086 (3.083)	0.646 (0.655)	0.849 (0.855)	1.052 (1.076)
Mean (of 9 specimens)						0.511 (0.506)	0.679 (0.675)	0.847 (0.844)
Average COV (of 9 specimens)						0.241 (0.213)	0.241 (0.215)	0.241 (0.216)

* - Values presented in brackets correspond to those obtained using Method II (Eq. 3)

Table 10 — Comparison of the results of probabilistic analysis of cracking moment* with the experimental values for built-up I-sections of Group I[30,32]

Specimen designation	Experimental cracking moment $(M_{cr})_{exp}$ (kN-mm)	Mean cracking moment $(\bar{X})$ (kN-mm)	Coefficient of variation	SK	CU	$\left(\frac{\bar{X}-1.64S}{(M_{cr})_{exp}}\right)$	$\left(\frac{\bar{X}}{(M_{cr})_{exp}}\right)$	$\left(\frac{\bar{X}+1.64S}{(M_{cr})_{exp}}\right)$
S1	638.827	441.238 (457.398)	0.139 (0.137)	0.252 (0.247)	3.091 (3.085)	0.533 (0.555)	0.849 (0.716)	0.691 (0.879)
S2	585.049	466.509 (480.334)	0.139 (0.138)	0.252 (0.248)	3.091 (3.086)	0.615 (0.636)	0.980 (0.821)	0.797 (1.006)
S3	422.987	433.628 (448.467)	0.139 (0.137)	0.252 (0.247)	3.091 (3.085)	0.791 (0.822)	1.260 (1.060)	1.025 (1.299)
S4	1180.624	1138.046 (1168.968)	0.139 (0.138)	0.252 (0.248)	3.091 (3.086)	0.743 (0.767)	1.184 (0.990)	0.964 (1.214)
S5	1180.221	1297.610 (1326.441)	0.139 (0.138)	0.252 (0.249)	3.091 (3.087)	0.848 (0.870)	1.351 (1.124)	1.100 (1.378)
S6	2520.679	2388.516 (2444.345)	0.139 (0.138)	0.252 (0.249)	3.091 (3.087)	0.731 (0.750)	1.164 (0.950)	0.948 (1.189)
S7	2550.541	2833.955 (2936.919)	0.139 (0.138)	0.252 (0.249)	3.091 (3.088)	0.872 (0.891)	1.389 (1.152)	1.131 (1.413)
Mean (of 7 specimens)						0.733 (0.756)	0.951 (0.976)	1.168 (1.413)
Average COV (of 7 specimens)						0.167 (0.162)	0.167 (0.163)	0.167 (0.163)

* - Values presented in brackets correspond to those obtained using Method II (Eq. 3)

Table 11 — Comparison of the results of probabilistic analysis of cracking moment* with the experimental values for built-up I-sections of Group II[30,32]

Specimen designation	Experimental cracking moment $(M_{cr})_{exp}$ (kN-mm)	Mean cracking moment $(\bar{X})$(kN-mm)	Coefficient of variation	SK	CU	$\left(\frac{\bar{X}-1.64S}{(M_{cr})_{exp}}\right)$	$\left(\frac{\bar{X}}{(M_{cr})_{exp}}\right)$	$\left(\frac{\bar{X}+1.64S}{(M_{cr})_{exp}}\right)$
A1	1476.908	1555.377 (1613.702)	0.142 (0.139)	0.251 (0.247)	3.091 (3.085)	0.809 (0.844)	1.053 (1.093)	1.298 (1.342)
A2	1626.498	1527.349 (1586.705)	0.142 (0.139)	0.251 (0.247)	3.091 (3.085)	0.721 (0.753)	0.939 (0.976)	1.157 (1.198)
A3	2071.469	1677.547 (1731.764)	0.142 (0.139)	0.251 (0.247)	3.091 (3.086)	0.622 (0.641)	0.810 (0.836)	0.998 (1.027)
B1	2662.905	3018.692 (2673.517)	0.224 (0.214)	0.123 (0.148)	3.180 (3.146)	0.717 (0.651)	1.134 (1.004)	1.550 (1.357)
B2	3381.997	3306.812 (3437.112)	0.224 (0.218)	0.123 (0.140)	3.180 (3.149)	0.619 (0.653)	0.978 (1.016)	1.337 (1.380)
B3	3267.642	3571.765 (3290.824)	0.224 (0.218)	0.123 (0.141)	3.180 (3.148)	0.692 (0.648)	1.093 (1.007)	1.495 (1.366)
C1	4753.043	5050.203 (3677.145)	0.100 (0.100)	0.206 (0.198)	3.056 (3.047)	0.890 (0.647)	1.063 (0.773)	1.236 (0.900)
C2	4549.633	5532.221 (3711.664)	0.100 (0.100)	0.206 (0.199)	3.056 (3.047)	1.018 (0.683)	1.216 (0.816)	1.414 (0.950)
C3	4010.328	5975.482 (3734.498)	0.100 (0.100)	0.206 (0.199)	3.056 (3.047)	1.248 (0.779)	1.490 (0.931)	1.733 (1.083)
Mean (of 9 specimens)						0.815 (0.700)	1.086 (0.939)	1.357 (1.178)
Average COV (of 9 specimens)						0.254 (0.106)	0.176 (0.115)	0.162 (0.163)

* - Values presented in brackets correspond to those obtained using Method II (Eq. 3)

Table 12 — Comparison of the results of probabilistic analysis of cracking moment* with the experimental values for monolithic I-sections[33,34]

Specimen designation	Experimental cracking moment $(M_{cr})_{exp}$ (kN-mm)	Mean cracking moment $(\bar{X})$ (kN-mm)	Coefficient of variation	SK	CU	$\left(\frac{\bar{X}-1.64S}{(M_{cr})_{exp}}\right)$	$\left(\frac{\bar{X}}{(M_{cr})_{exp}}\right)$	$\left(\frac{\bar{X}+1.64S}{(M_{cr})_{exp}}\right)$
MI1	2392.552	1917.708 (1997.001)	0.188 (0.184)	0.207 (0.209)	3.098 (3.089)	0.554 (0.583)	0.802 (0.835)	1.049 (1.087)
MI2	1550.598	1646.555 (1738.235)	0.188 (0.184)	0.207 (0.209)	3.098 (3.089)	0.734 (0.785)	1.062 (1.121)	1.390 (1.457)
MI3	4071.415	3072.792 (3145.855)	0.188 (0.184)	0.207 (0.211)	3.098 (3.094)	0.522 (0.539)	0.755 (0.773)	0.988 (1.006)
MI4	2184.589	2714.260 (2797.292)	0.188 (0.183)	0.207 (0.211)	3.098 (3.095)	0.859 (0.896)	1.243 (1.281)	1.627 (1.665)
MI5	4350.343	4863.236 (5096.013)	0.188 (0.183)	0.207 (0.209)	3.098 (3.090)	0.773 (0.819)	1.118 (1.171)	1.463 (1.524)
MI6	5514.691	5060.277 (5177.861)	0.188 (0.184)	0.207 (0.211)	3.098 (3.094)	0.634 (0.655)	0.918 (0.939)	1.201 (1.223)
Mean (of 6 specimens)						0.679 (0.713)	0.983 (1.020)	1.286 (1.327)
Average COV (of 6 specimens)						0.194 (0.197)	0.194 (0.198)	0.194 (0.199)

* - Values presented in brackets correspond to those obtained using Method II (Eq. 3)

1 The ratio between the probabilistic mean cracking moment $(\bar{X})$and experimental cracking moment,$((M_{cr})_{exp})$,for roofing and floor elements and, built-up and monolithic I-joists are computed and presented in Tables 8 – 12. The values of the average and coefficient of variation of the ratio $\frac{\bar{X}}{(M_{cr})_{exp}}$ for different types of elements considered are also furnished in these tables. Table 13 gives the average and coefficient of variation of the above ratio of all 37 specimens put together. These values for Methods I and II are, (0.940, 0.268) and (0.892, 0.214), respectively. Thus, it may be concluded that the probabilistic mean cracking moment compares satisfactorily with the experimental cracking moment. When comparisons are considered for elements of different cross-sections (Tables 8 – 12), the mean cracking moments compare satisfactorily with the experimental values except in case of floor elements (wherein the experimental cracking moment is underestimated by 32.1% when Method I is used and by 32.5% when Method II is used). Following a procedure similar to that presented in Ref. 39, it is concluded that the first-order approximation can be used in the determination of mean cracking moment. Therefore, the mean value of M_{cr} can be computed by substituting the mean values of the basic variables appearing im Eq. (1) or (3), depending on the method used to predict M_{cr}.

Table 13 — The agreement of experimental cracking moment with probabilistic mean and $(\bar{X} \mp 1.64S)$*

Quantity	Mean**	Standard deviation**	Coefficient of variation**
$\left(\frac{\bar{X}}{(M_{cr})_{exp}}\right)$	0.940 (0.892)	0.252 (0.191)	0.268 (0.214)
$\left(\frac{\bar{X}+1.64S}{(M_{cr})_{exp}}\right)$	1.089 (1.120)	0.283 (0.254)	0.259 (0.226)
$\left(\frac{\bar{X}-1.64S}{(M_{cr})_{exp}}\right)$	0.668 (0.664)	0.180 (0.139)	0.269 (0.210)

* - Values presented in brackets correspond to those obtained using Method II (Eq. 3)
** - Results of all 37 specimens are used in calculating different quantities

2 The average value of coefficient of variation of M_{cr} (of all specimens put together) is found to be 0.157 for Method I and 0.154 for Method II. Thus both the methods used to predict M_{cr} have given coefficient of variation of similar magnitude. Also, the coefficient of variation of M_{cr} (for a given type of element) is nearer to the coefficient of variation compressive strength of mortar

(Tables 7 and 8-12). This indicates that the statistical variations in cracking moment of ferrocement elements are mainly affected by the variations in compressive strength of mortar.

3 Knowing the mean and the standard deviation of M_{cr} (that is computed based on the values of coefficient of variation presented in Tables 8 -12), the ratios $\left(\frac{\bar{X}-1.64S}{(M_{cr})_{exp}}\right)$ and $\left(\frac{\bar{X}+1.64S}{(M_{cr})_{exp}}\right)$ are calculated to examine whether or not the $(\bar{X} \mp 1.64S)$ limits enclose the experimental cracking moment. These values for elements of different cross-section are also presented in Tables 8 -12. The average and coefficient of variation of these ratios are computed separately for different types of elements (Tables 8 – 12) and also for all elements considered together (Table 13).For the purpose ofillustration the results of probabilistic analysis by Method II only are shown in Fig. 8 for trapezoidal roofing elements. Similar plots have been made for specimens of other cross-sections also. In these figures the variations in non-dimensional quantity, $p_m\left(\frac{D}{L}\right)$, of different elements are represented on X-axis while Y-axis represents the non-dimensional quantity $\frac{M_{cr}}{f_{cu}\,bD^2}$ (where p_m is the ratio of area of mesh wires running in the longitudinal direction to the gross-section area, b is projected plan width of specimens, D is the total depth, f_{cu} is the compressive strength of mortar and L is the effective span). In the case of roofing elements (Fig. 8), the $(\bar{X} \pm 1.64S)$ limits enclose the $(M_{cr})_{exp}$ for all specimens except for the specimen K10-622. From similar plots of specimens of other types of cross-sections (not shown here) the following points are noted: (i) In the case of floor elements, it is observed that the $(\bar{X} \pm 1.64S)$ limits enclose $(M_{cr})_{exp}$ only for specimens F5 and F9. This is because the probabilistic mean cracking moments underestimate the$(M_{cr})_{exp}$ significantly for most of these specimens,,(ii) The experimental cracking moments of almost all built-up I-sections are within $(\bar{X} \pm 1.64S)$ and in the case of monolithic I-sections, they are enclosed within the limits for all the specimens. From the results presented in Tables 8 - 12, similar observations are made for Method I also. These comparisons show that the $(\bar{X} \pm 1.64S)$limits, in most of the cases, enclose $(M_{cr})_{exp}$. A summary of the results of comparison of all 37 elements put together is presented in Table 13.

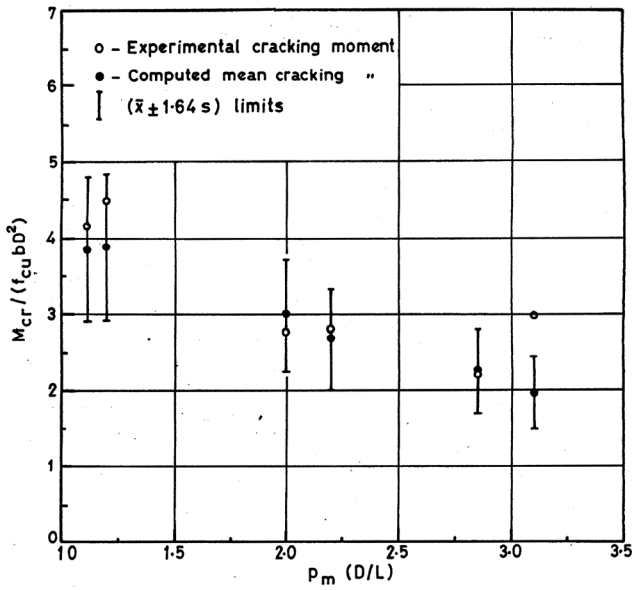

Fig. 8 — Comparison of experimental cracking moments with results of probabilistic analysis (Method – II) of trapezoidal roofing elements

4 It can be noted from Tables 8 – 12 that, for a given specimen, the coefficients of skewness and kurtosis of the distribution of cracking moment obtained using Methods I and II do not vary significantly. Already it has been pointed out that the coefficients of variation of M_{cr} estimated using both the methods are nearly the same. These observations indicate that the nature of distribution of M_{cr} remains almost the same for both the methods. The values of skewness coefficients (SK) of the distributions are slightly more than zero (implying longer falling tails) and kurtosis (CU) values are around 3.0. Since the values of SK and CU are nearer to zero and 3.0, respectively, cracking moment may follow a normal distribution. To get an idea about the nature of distribution of cracking moment histograms are drawn. For illustration, histogram of cracking moment obtained using Method II for specimen K20-422 only is shown in Fig. 9. Histograms of cracking moment for all other specimens of different types of cross-section considered are similar. From the histograms, it is noted that the distributions are almost symmetrical about the mean values (presented in Table 8 – 12). Chi-squaregoodness-of-fit

tests are performed to determine the actual distribution. Two hypothetical distributions considered for Chi-square tests are normal and beta. The allowable Chi-square values[39], used in Chi-square tests, for different degrees of freedom and for three confidence levels (namely 95%, 97.5% and 99%) that are commonly used in engineering decision making[39], are presented in Table 14. The computed Chi-square values for two hypothetical distributions considered are given in Table 15 for specimens K20-422, F1, S1, A1 and MI1 only for illustration (similar tables were prepared for other specimens also). It is noted from these tests that in the case of all the specimens both the distributions pass the Chi-square test criterion at 95% confidence level. However, in the present investigation a normal distribution is chosen to represent the statistical variations in M_{cr} (at 95% confidence level) since for this distribution standard tables are available and this distribution is convenient for mathematical treatment. A more rational distribution for M_{cr} is derived in Appendix A. This distribution (Eq. (A-7)), while making use of standard normal tables, avoids the possibility of cracking moment being negative (which theoretically may arise due to the assumption of a normal distribution for M_{cr}).

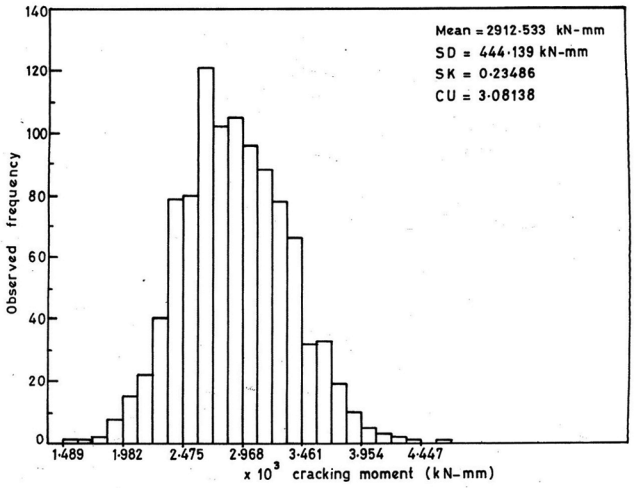

Fig. 9 — Histogram of cracking moment with results (Method – II) of the specimen K20-422 of trapezoidal crosssection

3 Results and Discussion

3.1 Determination of characteristic cracking moment

The cracking moment follows normal distribution and the values of coefficient of variation of M_{cr}

Table 14 — Allowable Chi-square values for different degrees of freedom[39]

Degrees of freedom	Allowable Chi-square values		
	At 95% confidence level	At 97.5% confidence level	At 99% confidence level
15	25.0	27.5	30.6
16	26.3	28.8	32.0
17	27.6	30.2	33.4
18	28.9	31.5	34.8
19	30.1	32.9	36.2
20	31.4	34.2	37.6

Table 15 — Chi-square test results of cracking moment (Method II) for elements of different cross-sections*

Specimen designation	Computed Chi-square values for		Remarks
	Normal distribution	Beta distribution	
K20-422	25.63 (16)	17.24 (17)	Both normal and beta distribution pass the test at 95% confidence level
F1	20.37 (16)	13.00 (17)	Both normal and beta distribution pass the test at 95% confidence level
S1	25.49 (16)	14.33 (16)	Both normal and beta distribution pass the test at 95% confidence level
A1	23.25 (16)	14.48 (16)	Both normal and beta distribution pass the test at 95% confidence level
MI1	15.10 (16)	11.65 (16)	Both normal and beta distribution pass the test at 95% confidence level

Note:

1. Values in brackets represent the degree of freedom related to Chi-square test.
2. * for the purpose of illustration results of specimen of each type of cross-section are presented here.
3. As can be seen from Tables 4 – 8, the statistical properties of cracking moment of different specimens in a group do not vary significantly. Hence the above Chi-square test results are valid for other specimens also.

obtained using Methods I and II are 0.154 and 0.157, respectively. Defining the characteristic cracking moment (M_{cr}^{*}) as 5% fractile of cracking moment distribution the same can be obtained from,

$$M_{cr}^{*} = (1 - 1.64 * 0.154) = 0.74\bar{X} \text{ (for Method I)} \quad \ldots (10)$$

$$M_{cr}^{*} = (1 - 1.64 * 0.157) = 0.75\bar{X} \text{(for Method II)} \quad \ldots (11)$$

Where $\bar{X}$is the mean cracking moment obtained by substituting the mean values of basic variables (Table 7) into Eq. (1) or Eq. (3), depending on the method used.

When a more rational probability density function of M_{cr} is used (Appendix A), the value of M_{cr}^{*} can be obtained from Eq. (A-9) by setting $F_{\bar{Y}}(y^{*})$ = 0.05 and determining the value of y^{*}.

4 Conclusion

From the studies reported in this paper the following points are noted:

1 The statistical properties and the probability density functions of diameter and ultimate strengths of weld mesh and steel bars (Table 7), determined in the present investigation, can be used in reliability analysis and reliability-based design of ferrocement flexural members.

2 Both the methods used to compute the cracking moment have given similar magnitudes of coefficient of variation of cracking moment. The coefficient of variation obtained for Methods I and II are 0.154 and 0.157, respectively. These values are approximately equal to the coefficient of variation of compressive strength of cement mortar and hence the statistical variations in compressive strength of cement mortar have significant effect on coefficient of variation of cracking moment.

3 For the variables considered in this study (Table 7), for both the methods used to estimate the cracking moment, cracking moment follows a normal distribution at 95% confidence level (Table 15).

4 Except in the case of channel-cross section floor elements, for almost all other specimens the experimental cracking moment is enclosed within $(\bar{X} \pm 1.64S)$limits (Table 13 and Fig. 8).

5 The characteristic cracking moment can be determined using Eq. (10) or (11), depending on the method used.The conclusion (4) also suggests that the characteristic cracking moment equation can be used in the design of ferrocement flexural members against first crack.

6 Based on the results obtained in this study, it is suggested that Method – II be used to predict the mean and characteristic cracking moment of ferrocement flexural elements. It is noted that Method – II takes into account the presence of mesh through mesh-mortar parameter (Eq. 4).

7 A more rational probability density and cumulative distribution functions derived in Appendix – A (Eqs. (A-7) and (A-9), respectively) can be used in the design decision making and in Monte Carlo simulation of cracking moment of ferrocement flexural elements.

Acknowledgements

The first author (KBR) did his Ph D under the guidance of the second author (PD). PD was also involved in formulation of the problem and had read almost all the contents of the paper. This paper is dedicated to the memory of PD. KBR is grateful to the management of ATRIA University where he is, at present, an adjunct faculty in the Centre of Excellence of Climate Sciences. He is very grateful to Dr V. Nagesh, founding Vice Chancellor of ATRIA University for his encouragement.

References

1 ACI Committee 549, *State-of-the-art report on ferrocement*, Concrete International Design and Construction, 4(8)(1982) 13.

2 ACI Committee 549R-97, *State-of-the-art report on ferrocement*, Concrete International Design and Construction, 4(8)(1997) 549R-1.

3 ACI Committee 549R-18, *Report on ferrocement*, American Concrete Institute (2018).

4 Naaman A E, *Ferrocement: a historical perspective*, FERRO-13, 13th International Symposium on Ferrocement and thin fiber reinforced inorganic matrices, Lyon, France, Editors : Amir S L & Hani N, (2021) 33.

5 Ahmed H A, Shahzada K & Fahad M, *Int J Dis Risk Red* 61(2021) 102341.

6 Arifujjaman Md, Paul I K & Raihan A, *Int J Eng Res & Tech* 10(4)(2021) 57.

7 *Ferrocement*, Proceedings of the Fifth International Symposium, UMIST, Manchester, U.K, Taylor & Francis, Editors: Nedwell P J & Swamy R N (1994).

8 Naaman A E, *Roman cement and ferrocement : Two coincidental discoveries of unparallel impact on modern construction*, FERRO – 14, 14th International Symposium on Ferrocement and thin Ultra High Performance (UHPC) Composites, Rutgers University – New Brunswick, NJ, USA (2024).

9 *Thin-Walled Structures: Research and Development*, Proceedings of the Second International Conference, National University of Singapore, Singapore, Editors: Shanmugam N E, Richard Liew J Y & ThevendranV, Elsevier (1998).

10 *Ferrocement technology*-WRD Handbook, (Maharastra Engineering Research Institute, Nashik), First Edition, 2018, 158p.

11 Madhava Rao A G, Ramachandra Murthy D S & Annamalai G, *Modern trends in housing in developing countries* (E& FN Spon), 1984, 380p.

12 Lugowski J, *Ferrocement super-insulated shell house design and construction*, Master's degree project in Energy Technology, Stockholm, Sweden, 2013.

13 Paul B K & Pama R P, *Ferrocement* (International Ferrocement Centre, Asian Institute of Technology, Bangkok, Thailand), Edition :1978, 149p.

14 Naaman A E, "Ferrocement and Thin Reinforced Cement Composites: Five Decades of Progress", Proceedings of 12th International Symposium on Ferrocement and Thin Cement Composites, Belo Horizonte, Brazil, Editors: Rodriguez C, Savio Nunes Bonifacio, Naaman A E &Wainstock Rivas H, Brasilain Ferrocement Society (2018).

15 Naaman A E, *Ferrocement and Laminated Cementitious Composites* (Techno Press), ISBN 0-9674939-0-0, 2000.

16 Naaman A E, *Ferrocement: International Revival*, Proceedings of ACI Symposium on Concrete Materials Science to Applications, a tribute to S P Shah, ACI SP-206, Editors: P Balaguru & W Weiss, (2002) 323.

17 Naaman A E, *Arab J Sci Eng* 37(2012) 421.

18 Naaman A E, *Ferrocement: Progress review and critical need for the future*, FERRO-11 International Symposium on Ferrocement and 3rd ICTRC International Conference on Textile Reinforced Concrete : Aachen, Germany, Brameshuber, Editor: Wolfgang (2015).

19 Shah S P, *A perspective on fibers, ferrocement and UHPC*, FERRO – 14, 14th International Symposium on Ferrocement and thin Ultra High Performance (UHPC) Composites, Rutgers University – New Brunswick, NJ, USA (2024).

20 *Ferrocement Model Code, Building Code Recommendations for Ferrocement* (IFS 10 – 01), International Ferrocement Society, www.ferrocement.ifs.com, 2001.

21 Minde P, Bhagat D, Patil M & Kulkarni M, *Mat Today* (2023).

22 Gandhomi A H, Roke D A & Sett K, *Eng Struct*, 57(2013) 169.

23 Naderpour H, Eidgahee D R, Fakharian P et al., *Eng Sci Tech*, 23(2)(2020) 382.

24 Behnia A, Ranjbar N, Chai H. K & Masaeli M, *Const Build Mat,* 122(2016) 823.

25 Pyzer-Knapp E O, Pitera J W, Staar P W J, Takeda S, Laino T, Sanders D P, Sexton J, Smith J R & Curioni A, *npj Comput Mat*, 8(84)(2022) 1.

26 Li Z, Yoon J, Zhang R, Rajabipour F, Srubar W V, Dabo I & Radlinska A, *npjComput Mat*, 8(127)(2022) 1.

27 Kazemi R, *Eng Rep*, 5(e12676)(2023) 1.

28 Desayi, P and Ramesh, N. L., "Tests on ferrocement channel units", Nervi International Symposium on Ferrocement, RILEM, 22 – 24 July 1981, Bergamo, Italy, pp. 2169 – 2177.

29 Desayi P, Viswanatha C S &Kanappan S, *J Ferro*, 12(3)(1982) 273.

30 Desayi P, Senthil Nathan A &Maheedhar Reddy Y, *J Inst Eng (India)*, 65(CI5)(1985) 215.

31 Senthilnathan A, *Application of ferrocement to roofing joists*, M.E. Dissertation, Indian Institute of Science, Bangalore, 1981.

32 Maheedhar Reddy M, *Ferrocement I – Joists*, M.E Dissertation, M.E. Dissertation, Indian Institute of Science, Bangalore, 1982.

33 Balaji Rao K, *Studies on Reliability of Reinforced Concrete Beams in Cracking and Ferrocement Elements in Tension and Flexure*, Ph.D Thesis, Indian Institute of Science, Bangalore, 1990.

34 Desayi P & Balaji Rao K, *Prediction of cracking and ultimate moments and load-deflection behaviour of ferrocement elements*, Proceedings, Third International Symposium on Ferrocement, New Delhi, (1988) 90.

35 Desayi P & Balaji Rao K, *J Struct Eng (CSIR-SERC),* 49(6)(2023) 445.

36 Balaji Rao K &Desayi P, *Ind J Eng & Mat Sci*, 30(2023) 530.

37 Balaji Rao K and Desayi P, *Eco-friendly brittle matrix composite in direct tension - determination of upper and lower bounds for ultimate loads*, Advances in Risk and Reliability Modelling and Assessment. ICRESH 2024. Lecture Notes in Mechanical Engineering. Springer, Singapore, Editors: Varde P V, Vinod G & Joshi N S (2024) 871.

38 Desayi P & Balaji K Rao, *Int J Cem Comp & Ligh Conc*, 10(1)(1988) 15.

39 Ang A H-S & Tang W H, *Probability Concepts in Engineering Planning and Design, Vol. I* (John Wiley and Sons, New York), 1975, 409p.

40 Milik Tichy & Milos Vorlicek, *Statistical theory of concrete structures, with special reference to ultimate design* (Irish University Press, Shannon, Academia, Prague), 1972.

41 Ellingwood B R, *J Struct Div Proc ASCE*, 105(ST4) (1979) 713.

42 Ranganathan R & Dayaratnam P, *J Inst Eng (India)*, 58(CI2)(1977) 20.

43 Mirza S A &Mac Greogor J G, *ACI J*, 76(11)(1979) 1159.

44 Mirza S A &Mac Greogor J G, *Can J Civ Eng*, 9(1982) 431.

45 Mirza S A & Mac Greogor J G, *J Struct Eng, Proc. ASCE*, 105(ST5)(1979) 921.

46 Papoulis A & Pillai U, *Probability – Random Variables and Stochastic Processes* (McGraw Hill Education), 4th Edition, 2017, 872pp.

Appendix – A

Determination of more rational probability density and cumulative distribution functions of the cracking moment (M_{cr})

In this Appendix, an attempt is made to determine a more rational pdf of M_{cr}. From the probabilistic analysis

of cracking moment presented in Section 2, it is noted that the statistical variations in compressive strength of mortar has significant effect on the statistical variations of cracking moment. It is observed from Table 3, that the compressive strength of mortar cube follows a normal distribution. Theoretically, the range space of normal distribution is (-∞,∞). The negative values of the compressive strength do not have any engineering significance. Also, the negative compressive strength values pose difficulties in the computation of modulus of rupture of mortar. The possibilities of realizing negative values of normal distribution is more pronounced in the case poor quality control in the production mortar. To overcome this difficulty, a more rational theoretical probability density function of cracking moment is derived below. The cumulative distribution function so derived can be used to estimate the characteristic cracking moment used in the design.

Based on the comparison of computed M_{cr} with the respective experimental M_{cr} of 37 specimens (presented in Section 2.2), Method – II is recommended for the estimation of M_{cr} of ferrocement flexural elements. Accordingly, the cracking moment of ferrocement flexural member can be estimated using Eq. (3). The corresponding characteristic cracking moment, knowing that M_{cr} follows normal distribution (Section 2.4.1), can be determined using Eq. (6). However, due to the afore mentioned reasons a new design criterion, which is more practical, is obtained by observing that M_{cr} is a function of the significant basic random variable, f_{cu} (conclusion 1). Since dimensional variations and other strength variations (presented in Table 7) are considered as non-random, it is assumed that the probabilistic variations in f_{cu} and f_{cm} (Eq. (4)) are same. This is a reasonable assumption since effects of dimensional and strength of mesh wires- variations on M_{cr} variation is small. Equation (3) can be written as,

$$M_{cr} = \frac{0.57\sqrt{f_{cm}}\, I_g}{y_b} = C\sqrt{f_{cm}} \quad \ldots \text{(A-1)}$$

Where

$C = \frac{0.57 I_g}{y_b}$ is a constant for a given flexural member since dimensional variations are neglected. Letting X represent the random variable f_{cm} and Y the random variable M_{cr} Eq. (A-1) can be written as

$$Y = C\sqrt{X} \quad \ldots \text{(A-2)}$$

Wherein the pdf of X is given by,

$$f_X(x) = \left[\frac{1}{\sigma\sqrt{2\pi}} e^{\left\{\frac{-1}{2}\left(\frac{x-\mu}{\sigma}\right)^2\right\}}\right]; \quad -\infty < x \leq \infty \quad \ldots \text{(A-3)}$$

Where μ = mean mesh-mortar cube compression strength and σ is the standard deviation of mesh-mortar cube compression strength.

Due to the considerations presented earlier, a doubly truncated pdf is considered for representing mesh-mortar cube compression strength. Accordingly the pdf of $\tilde{X}$ is given by,

$$f_{\tilde{X}}(\tilde{x}) = K\left[\frac{1}{\sigma\sqrt{2\pi}} e^{\left\{\frac{-1}{2}\left(\frac{\tilde{x}-\mu}{\sigma}\right)^2\right\}}\right]; \quad x_{min} < \tilde{x} \leq x_{max} \quad \ldots \text{(A-4)}$$

Where K is the normalization constant such that $\int_{x_{min}}^{x_{max}} f_{\tilde{X}}(\tilde{x})\, d\tilde{x} = 1$. After some algebraic calculations, the value of K can be computed from,

$$K = \frac{1}{\left[\Phi\left(\frac{x_{max}-\mu}{\sigma}\right) - \Phi\left(\frac{x_{min}-\mu}{\sigma}\right)\right]} \quad \ldots \text{(A-5)}$$

Where Φ(.) is cumulative distribution function of standard normal variate. Typically for $x_{min} = \mu - 3\sigma;\ x_{max} = \mu + 3\sigma$, the value of K is obtained as 1.003 while for $x_{min} = \mu - 2\sigma;\ x_{max} = \mu + 2\sigma$, the value of K is 1.048. Thus, the above pdf gives flexibility to the design decision maker with regard to bounds preferred depending on quality control in mortar mix production.
Now, the modified random cracking moment, $\tilde{Y}$, is given by,

$$\tilde{Y} = C\sqrt{\tilde{X}};\ \ C\sqrt{x_{min}} < \tilde{y} \leq\ C\sqrt{x_{max}} \quad \ldots \text{(A-6)}$$

Using the Jacobian method of determination of pdf of function of random variable[46] the pdf of $\tilde{Y}$ is given by,

$$f_{\tilde{Y}}(\tilde{y}) = \left[\frac{1}{\sigma K\sqrt{2\pi}} \frac{2\tilde{y}}{C^2} e^{\left\{ \frac{-1}{2}\left(\frac{\frac{\tilde{y}^2}{C^2} - \mu}{\sigma} \right)^2 \right\}} \right];\quad C\sqrt{x_{min}} < \tilde{y} \leq\ C\sqrt{x_{max}} \quad \ldots \text{(A-7)}$$

The cumulative distribution function of M_{cr} is given by,

$$F_{\tilde{Y}}(y^*) = \int_{C\sqrt{x_{min}}}^{y^*} f_{\tilde{Y}}(\tilde{y})\, d\tilde{y} \quad \ldots \text{(A-8)}$$

It can be shown that

$$F_{\tilde{Y}}(y^*) = \frac{1}{K}\left[\Phi\left(\frac{\left(\frac{y^*}{C}\right)^2 - \mu}{\sigma} \right) - \Phi\left(\frac{x_{min} - \mu}{\sigma} \right) \right];\ C\sqrt{x_{min}} < \tilde{y} \leq\ C\sqrt{x_{max}} \quad \text{(A-9)}$$

With $F_{\tilde{Y}}\left(C\sqrt{x_{min}}\right) = 0\ and\ F_{\tilde{Y}}\left(\ C\sqrt{x_{max}}\ \right) = 1$. One of the important features of the model (Eq. (A-9)) is that the range space of pdf of M_{cr} is always positive and the quality control in the production of mortar can be incorporated by specifying x_{min} (i.e. minimum expected compression strength of mortar). Also, for a given value of $F_{\tilde{Y}}(y^*)$which is generally 0.05 (useful in arriving at characteristic value of M_{cr}), and x_{min} , y^*can be determined. This gives flexibility to the designer to include information on quality control of mortar production and any specified value of $F_{\tilde{Y}}(y^*)$. It is to be noted that the values of μ and σ can be obtained using the first order approximation of Eq. (A-1).